Nanomed Res J 8(2):193-209, Spring 2023

RESEARCH ARTICLE

Electrospun kefiran biocomposite nanofibers as a novel transdermal carrier of pramipexole

Fatemeh Mehrali[1], Hakimeh Ziyadi[1*], Malak Hekmati[1], Reza Faridi-Majidi[2], Mahnaz Qomi[3]

[1] Department of Organic Chemistry, Faculty of Pharmaceutical Chemistry, Tehran Medical Sciences, Islamic Azad University, Tehran, Iran

[2] Department of Medical Nanotechnology, School of Advanced Technologies in Medicine, Tehran University of Medical Sciences, Tehran, Iran

[3] Active Pharmaceutical Ingredients Research Center, Tehran Medical Sciences, Islamic Azad University, Tehran, Iran

ARTICLE INFO

Article History:
Received 26 Dec 2022
Accepted 19 Mar 2023
Published 01 May 2023

Keywords:
Composite nanofibers
Electrospinning
Kefiran
Pramipexole
Chitosan

ABSTRACT

The nanostructures of kefiran can be used in different applications such as medicine, drug delivery and biology. Aiming to introduce a novel biocomposite of kefiran usable in drug delivery systems, the biocomposite nanofibers of kefiran/chitosan/poly (vinyl alcohol) (Kf/CS/PVA) were prepared with a bead-less morphology and minimum mean fiber diameter. The optimum concentration of polymers, blend ratios, and electrospinning parameters were chosen based on analyzing the nanofibers by the scanning electron microscope (SEM). The prepared nanofibrous mats were then characterized further with the atomic force microscope (AFM), Fourier transform infrared (FT-IR) and contact angle measurement. The prepared nanocomposite was studied as a potential drug carrier for pramipexole dihydrochloride, a widely used treatment for Parkinson's disease. Pramipexole loaded Kf/PVA and Kf/CS/PVA nanocomposite were fabricated using electrospinning and crosslinked by glutaraldehyde. The release features of all drug-loaded nanofibers were conducted for studying using in vitro dissolution procedure and UV-Visible spectroscopy. Kf/PVA nanofibers showed slow and low drug release properties in contrast to Kf/CS/PVA. Although crosslinked composite nanofibers had slower release behavior than their non-cross-linked counterparts. The maximum release and reaching a steady state of crosslinked Kf/CS/PVA took four days introducing it as the best candidate of kefiran nanocomposite for drug delivery of pramipexole.

How to cite this article
Mehrali F., Ziyadi H., Hekmati M., Faridi-Majidi R., Qomi M. Electrospun kefiran biocomposite nanofibers as a novel transdermal carrier of pramipexole. Nanomed Res J, 2023; 8(2): 193-209. DOI: 10.22034/nmrj.2023.02.009

INTRODUCTION

Natural polymers (biopolymers) are used as nontoxic, biodegradable, and biocompatible materials, but they are poor in mechanical performance compared with synthetic polymers. The properties of biopolymers such as tensile strength, break elongation, and stiffness can be improved by adding synthetic polymers and producing biocomposites [1-4]. Polysaccharide-based bio-nanocomposites with animal and plant origins (e.g., chitosan, cellulose, kefiran, and starch) can be blended with different synthetic polymers (e.g., polyvinyl alcohol and polyethylene oxide) in order to prepared biocomposites with improved properties [5-8].

As a natural carbohydrate polymer taken from kefir grains, Kefiran (Kf) has gained significance among biopolymers owing to its role in fermented products and applications as a vehicle for probiotic microorganisms, packaging food, and oral delivery of some drugs [9-12]. Additionally, kefiran and kefiran composites have been reported to have numerous health promotion

* Corresponding Author Email: *behnazziyadi@yahoo.com*

effects such as antitumor, antifungal, antibacterial activities, and neuroprotection effects as well as kefir was introduced as a protective dietary supplementation against viral infection with the inhibitory action of the 'cytokine storm' (leading protection from the COVID-19 disease) [13-21]. Such benefits make kefiran a plausible choice for developing new nanostructured materials. Pure kefiran films are generally brittle with a lackluster mechanical performance. Limited research has reported mixing kefiran with plasticizers or polymers to enhance films' transparency, flexibility, and mechanical resistance [22-25]. Producing a novel nanocomposite of kefiran with improved mechanical and morphological properties is a challenge for kefiran product studies as nanomedicine materials. Enhanced flexibility without tensile strength impairment and good blend miscibility is already shown in Kf/starch composite films [26]. Improved physical and mechanical composite properties are reported by the addition of whey protein isolate [27], cellulose gum (CMC) [28], and waterborne polyurethane [29] to kefiran films.

From kefiran nanostructures, kefiran nanofibers fabricated by electrospinning method using water as green solvent is also reported [30], and since then, some studies have been published to produce nanocomposites of kefiran nanofibers with a potential ability to be used in several nanomedicine fields, from drug delivery to regenerative medicine and tissue engineering. For example, Jenab et al. fabricated Kf/PAN nanofibers showing that kefiran nanofibers are applicable to enhance the growth of PBMC and reduce the growth of MCF7 cancerous cells [31]. The Kf/PAN nanofibrous scaffolds have been found to have superior properties for the neural stem cell culture, particularly for fixing injured spinal cords. Kf/polyethylene oxide (PEO) nanofibers' antimicrobial properties with oxidizing functional groups fabricated by the electrospinning method are also confirmed against *S. aureus* [32].

Among many types of synthetic polymers, polyvinyl alcohol (PVA) is a promising polymer for producing of nanofibrous composite due to its water-soluble, noncorrosive, biocompatible, and biodegradable properties [33-34]. The bionanocomposites of PVA are promised carriers for medication in diagnosis, drug delivery system, sensing, and actuation in a living organism because of their suitable chemical and biological resistance, high tensile and hydrophilic strength, and strong fiber formation power [35-38]. Previously, our research team investigated the novel Kf/PVA nanofibers [39] and kefiran/PVA/PVP nanofibers [40], and it was observed that kefiran can produce smooth and fine composite nanofibers with PVA.

Also, Faridi et al. [41] fabricated composite nanofibers of kefiran with chitosan (CS) which is a linear water-insoluble biopolymer and has outstanding properties such as non-toxicity, biodegradability, and biocompatibility used to prepare water insoluble composites [42-46]. It is found that increasing the amount of CS polymer in kefiran's composite films can lower moisture content and solubility in water but can increase tensile and puncture strength and break elongation [47]. So, CS can be a good water-insoluble biopolymer to control the solubility of Kf composite nanofibers.

Kefiran has gained significance in therapeutic applications such as novel drug delivery nanocarriers, tissue engineering scaffolds, and platelets encapsulation [48]. Despite the enormous potential of kefiran in medicine as well as application of nanofibers in transdermal drug delivery systems, limited research has studied kefiran nanofibers in drug delivery systems. To the best of the authors' knowledge, only the delivery of antibiotic agents such as Kf/doxycycline nanofiber [48] and Kf/ciprofloxacin microdpher [49] have been investigated thus far. And no single study has reported using kefiran nanofibers as a drug delivery carrier for other therapeutic agents. Although the applications of Kf/PVA [39-40] and Kf/CS [41] composite nanofibers in drug delivery have yet to be explored.

Accordingly, in this study, we prepared and characterized kefiran-based biocomposite nanofiber mats using PVA and CS polymers to the delivery of pramipexole. First, the electrospinning method was used to fabricate Kf/CS/PVA composite nanofibers with a unique morphology and a large, specific surface area. The chemical, physical, and morphological properties of prepared nanocomposites were then characterized and discussed. Moreover, the addition of the pramipexol drug to Kf/CS/PVA nanofibers and its drug release properties were investigated and compared with Kf/PVA nanofibers, promising to introduce novel biocomposite patches based on kefiran nanofibers to be used in medicine and drug delivery systems in neurological drugs delivery.

EXPERIMENTAL

Materials and apparatus

Kefir grains were purchased from a grocery store in Tehran, Iran. PVA (88,000 g/mol molecular weight and 88% degree of hydrolysis) and chitosan (deacetylation degree of 75%) were obtained from Sigma-Aldrich (USA). 240 mg of pramipexole dihydrochloride were applied. All solvents and chemicals were used as received.

The electrospinning processes were carried out using a laboratory scale electrospinning unit, Electronics (FNM Ltd., Iran, http://www.fnm.ir), with high DC voltage power supplies (0-35 kV) and a syringe with an 18-gauge stainless steel needle as the nozzle. The electrospun nanofibers were collected on an aluminum foil wrapped on a cylindrical rotating collector. Fourier transform infrared (ATR-FTIR) spectra were recorded at the spectral range of 400-4000 cm^{-1} with Shimadzu equipped with an attenuated total reflectance diamond crystal accessory. Thermal analyses were carried out employing the differential scanning calorimetry (DSC) method with a METTLER TOLEDO DSC1 STAR^e system. The morphologies of the fibers were characterized by the scanning electron microscope (SEM, Philips XL 30, and S-4160). The obtained electrospun mats which were collected on aluminum foil were cut into 3×3 cm pieces, coated with gold by a sputter coater (Bal-Tec, SCD 005, USA), and then SEM images were recorded. The mean diameter of nanofibers was estimated to be over 20 nanofibers by the Microstructure Measurement software. Nanofiber diameter distributions were analyzed using the Origin software. Atomic force microscope (AFM) measurements were carried out by AFM NT-MDT, TD150 (Russia). UV spectra were recorded using a UV-Visible spectrophotometer PG Instrument T80. *In-vitro* dissolution tests of electrospun mats were performed using a USP dissolution apparatus I (IRAN, www.noavaranInd.co). Contact angles were measured using a Veho USB Microscope 400x.

Preparation of kefiran biopolymer solutions

Kefiran polysaccharide was extracted from kefir grain and cultured in milk using the previously reported method [42]. Briefly, kefir grains were cultured in skimmed milk for 24 hours at room temperature. Then, the grains were washed gently with water followed by another culturing cycle, and cycles were repeated every day for one month. The accurate weight of activated kefir grains was added to boiling water (1:10) and stirred for two hours. The resulting mixture was cooled to 20°C. The dissolved polysaccharide in the supernatant was precipitated by adding two volumes of cold ethanol (96%) and kept at -20 °C for 24 hours. Next, the mixture was centrifuged at 4 °C. The resulting precipitate was finally dissolved in warm distilled water (the kefiran solution) and then dried in an oven at 60 °C for 48 h. 2%, 4%, 6%, and the 8% kefiran solutions were prepared by adding 0.2, 0.4, 0.6, and 0.8 g kefiran into 10 mL of distilled water; finally, the resulting solutions were magnetically stirred at 50 °C for one hour.

Preparation of Kf/CS/PVA composite fibers

Kf/CS/PVA composite fibers by varying the concentration of kefiran

To prepare the 3% W/V CS solution, 0.6 g of CS was slowly added to 20 mL of diluted acetic acid (1% V/V in water) as solvent while stirring for 30 minutes.

10 % W/V of PVA was prepared by slowly dissolving of 1g PVA in 10 mL 50 °C water during 1h.

CS/PVA solution was prepared with mixing ratio of 30:70 for prepared solutions of CS:PVA.

Various concentrations of kefiran solution in water (2, 4, 6, and 8 % W/V) were prepared then added to CS:PVA with a mixing ratio of 50:50, and 5 mL of these solutions were loaded into a syringe. The syringe was connected to the syringe pump of Electroris. The optimum electrospinning conditions of this experiment were set as follows: a voltage of 15 kV, 0.5 mL/h flow rate, and 10 cm for tip-to-collector distance. Morphology and the size of electrospun nanofibers were determined via SEM.

Kf/CS/PVA composite fibers by varying the polymer mixing ratios

To determine the optimum ratio of kefiran solution to CS/PVA solutions, four mixtures were prepared (as 10:90, 25:75, 50:50, 75:25, and 90:10). The electrospinning conditions of this experiment were set as mentioned in the previous section (2.3a). Morphology and the size of electrospun nanofibers were determined via SEM.

Optimized Kf/CS/PVA composite solution

Kf:CS/PVA (10:90, optimal mixing ratio gained from analysis of 2.3b nanofibers) were prepared by adding 4.5 mL of PVA:CS solution (70:30) to

0.5 mL of 8% (W/V) kefiran solution (optimal concentration of kefiran gained from analysis of 2.3a nanofibers) in water, and the mixture was dissolved under magnetic stirring at 50 °C until a clear solution was obtained. The solution was cooled to room temperature.

Preparation of pramipexole-loaded Kf/CS/PVA nanofibers

240 mg pramipexole was gradually added to 5 mL Kf/CS/PVA solution (prepared according to 2.3c) of and stirred for 15 minutes. 10 mL of this solution was loaded into the syringe to be electrospun under the electrospinning conditions of section 2.3a.

To crosslink nanofibers in presence of glutaraldehyde vapor, a 10×15 cm piece of pramipexole-loaded Kf/CS/PVA electrospun mat was placed in a desiccator containing 20 mL glutaraldehyde for 24 hours, and then, this section was dried in vacuum for four hours at room temperature to remove the glutaraldehyde residual. This piece and a non-cross-linked sample of the same size were later analyzed for evaluating *in vitro* drug release properties by dissolution test and UV-Visible spectroscopy.

Preparation of Pramipexole-loaded Kf/PVA nanofibers

6 mL PVA solution with a concentration of 8% W/V was added to 4 mL Kf solution with a concentration of 6% W/V (60:40 mixing ratio according to previously reported data [39]), and the mixture was stirred at 50°C until a clear solution was gained. Then, the solution was cooled to room temperature and pramipexole dihydrochloride (240 mg) was added gradually over time. 10 mL of this solution was electrospinned when the conditions were set as follows: an applied voltage of 18 kV, 1 mL/h flow rate, and 200 mm tip-to-collector distance.

A 15×10 cm piece of pramipexole-loaded Kf/PVA mat was cross-linked via the same procedure as explained in the previous section. Pramipexole-loaded Kf/PVA and cross-linked pramipexole-loaded Kf/PVA were analyzed for evaluating *in-vitro* drug release properties by dissolution test and UV-Visible spectroscopy.

In-vitro drug release measurements

Standard solutions of 1, 2, 5, 10, 15, 20, and 25 ppm of pramipexole drug were made. Then, the absorbance of standard solutions was measured at a maximum wavelength of 263 nm according to pramipexole United States Pharmacopeia (USP) using distilled water as a blank solution. A calibration curve was drawn as a plot of absorbance vs. concentration. Crosslinked and non-crosslinked pramipexole-loaded nanofibrous mats (Kf/PVA and Kf/CS/PVA) were chopped and placed in separate dissolution baskets containing 900 mL phosphate buffer (pH 7.4) maintained at optimal temperature 37 °C and stirred at 100 rpm. Samples (5 mL) were withdrawn after 5, 10, 20, and 30 minutes and after 1, 2, 6, 24, 48, and 72 hours from the medium release, and the fresh buffer at an equivalent volume was replaced immediately. The released drug concentrations in the samples were assayed by UV-Visible spectroscopy.

RESULTS AND DISCUSSION

Kefiran polysaccharide was extracted from activated kefir grains in skimmed milk (Fig. 1). The effect of the concentration of kefiran solution (% W/V) on the morphology of Kf/CS/PVA composite nanofibers was examined. A solution of CS:PVA (30:70) was prepared, and then, this solution was mixed with different concentrations of kefiran solutions with a ratio of 50:50 (Table 1).

As depicted in the SEM images of Fig. 2, all samples had nanofibrous morphologies; however, samples a-c had discontinuous fiber formation. The mean diameter of the fibers decreased with an increase in the concentration of kefiran. Sample d with 8% W/V of kefiran concentration showed fibers with the lowest mean diameter, smooth, uniform, and continuous fiber formation with a small amount of bead, hence chosen as the optimum kefiran concentration. The optimum blending ratio of kefiran solution (8% W/V) to CS:PVA polymeric solutions (10% W/V PVA and 3% W/V CS with the blending ratio of 30:70) was determined by comparing five different blending ratios (Table 2).

Fig. 3 demonstrates the Kf/CS/PVA composite nanofibers' SEM images and fiber diameter distribution relating to different blending ratios of Kf:CS/PVA. The mean diameter of the nanofibers enhanced with increasing kefiran ratio in polymer blends. At high Kf ratios ranging from 25-90 % V/V adhesion between nanofibers, noncontinuous electrospinning, and lack of uniformity in the distribution of diameters were observed (Fig. 3 (b-e)). At the 10 % V/V Kf ratio in a polymeric blend

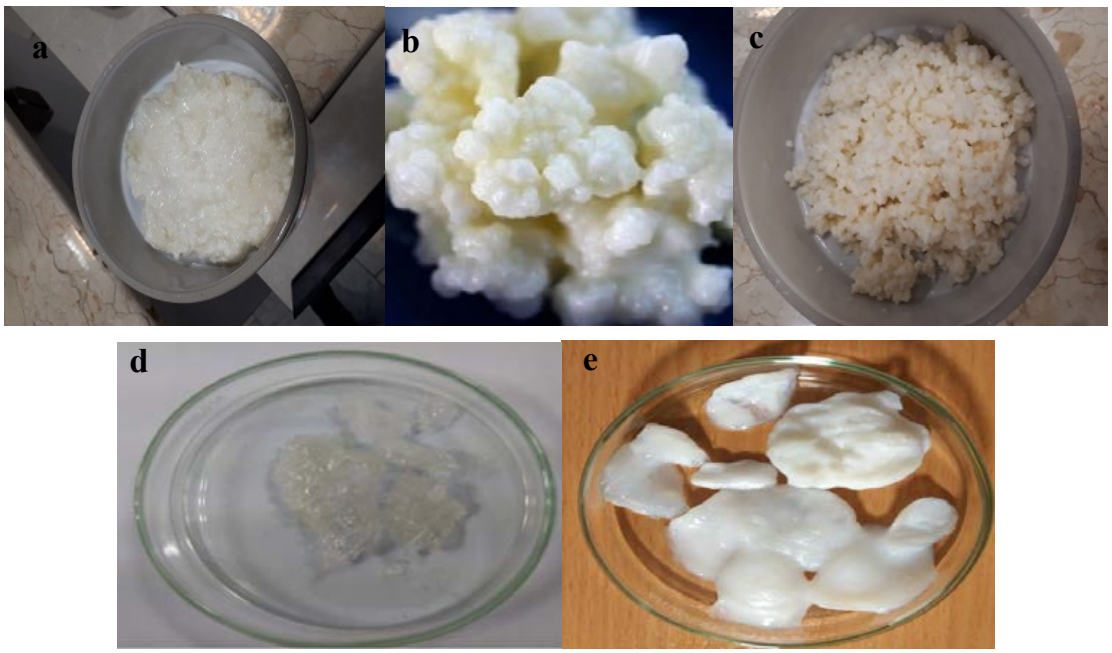

Fig. 1. Macroscopic image of (a) kefir grains (b) kefir (c) cultured grains in skimmed milk (d) dried kefiran (e)As-extracted kefiran.

Table 1. Investigation of fiber structures of Kf/Cs/PVA[a] samples, which correspond to different concentrations of kefiran solution[b].

Entry	Concentration of kefiran solution (w/v %)	Mean fibers diameter (nm)	Fiber structure
Sample a	2	87	discontinuous fibers
Sample b	4	59	Inconsistent fibers
Sample c	6	74	Inconsistent fibers
Sample d	8	30	Uniform and Continuous fibers

[a] Blending ratio of Kf:Cs/PVA is 50:50.

[b] Electrospinning parameters were kept constant (an applied voltage of 15 kV, 0.5 mL/h flow rate, temperature of around 25-30°C, 10 cm tip-to-collector distance).

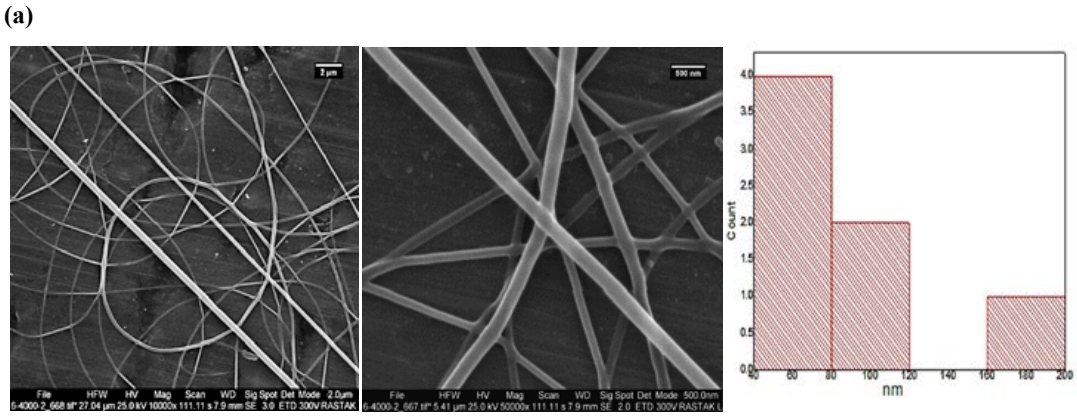

Fig. 2. SEM images (with different magnification, scale bar corresponds to 2 µm and 500 nm) and fiber diameter distribution of Kf/Cs/PVA nanofibers relating to different kefiran solution concentrations: (a) 2% (b) 4% (c) 6% (d) 8% W/V.

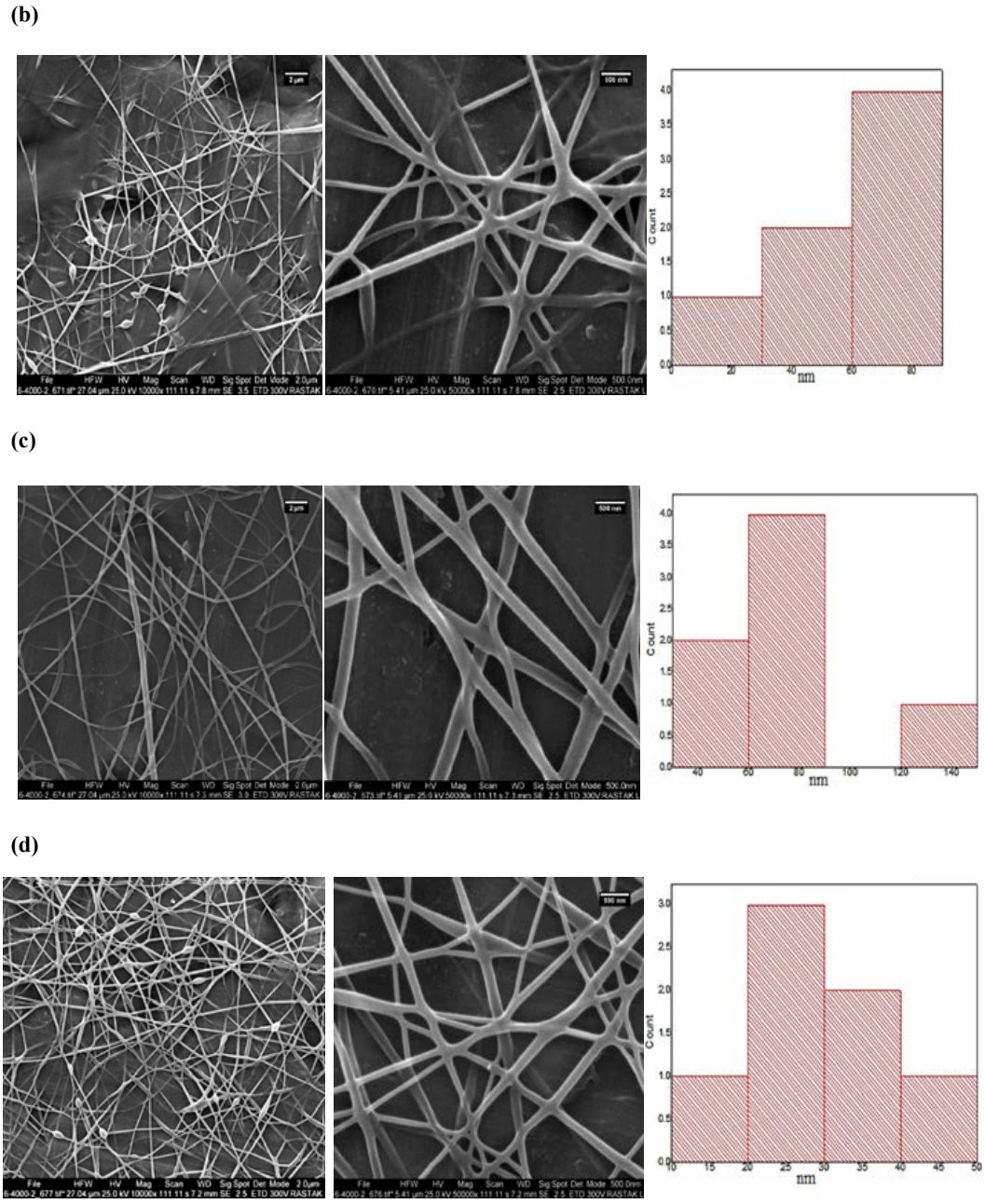

Continued Fig. 2. SEM images (with different magnification, scale bar corresponds to 2 µm and 500 nm) and fiber diameter distribution of Kf/Cs/PVA nanofibers relating to different kefiran solution concentrations: (a) 2% (b) 4% (c) 6% (d) 8% W/V.

Table 2. The effect of polymeric blending ratios of Kf/Cs/PVA[a] samples on average fiber diameters.

Entry	kefiran ratio (V/V)	blending ratio of PVA: Cs (V/V)	Average fibers diameter (nm)
Sample a	10	90	125
Sample b	25	75	150
Sample c	50	50	138
Sample d	75	25	183
Sample e	90	10	158

[a] Electrospinning parameters were kept constant (an applied voltage of 15 kV, 0.5 mL/h flow rate, temperature of around 25-30°C, 10 cm tip-to-collector distance).

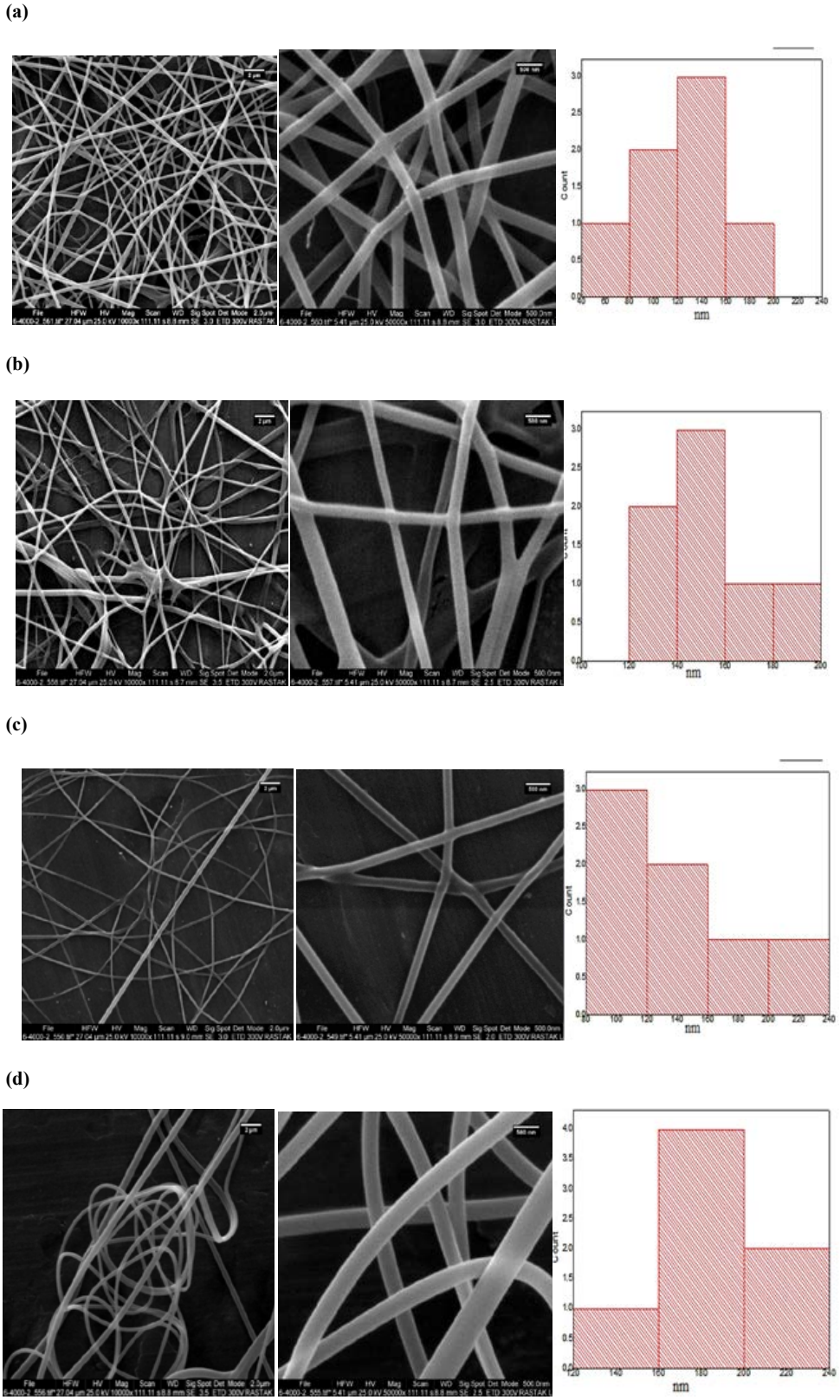

Fig. 3. SEM images (with different magnification, scale bar corresponds to 2 μm and 500 nm) of Kf/Cs/PVA nanofibers corresponding to different polymeric blending ratios of Kf:Cs/PVA: (a) 10:90 (b) 25:75 (c) 50:50 (d) 75:25 and (e) 90:10.

(e)

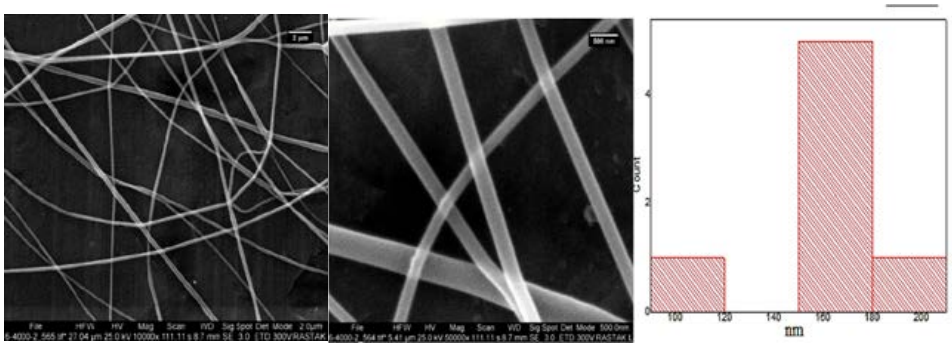

Continued Fig. 3. SEM images (with different magnification, scale bar corresponds to 2 μm and 500 nm) of Kf/Cs/PVA nanofibers corresponding to different polymeric blending ratios of Kf:Cs/PVA: (a) 10:90 (b) 25:75 (c) 50:50 (d) 75:25 and (e) 90:10.

of CS/PVA:Kf, the lowest mean diameter, beadless and continuous fiber structures were obtained (Fig. 3a).

Therefore, nanofibrous mats comprising Kf:CS/PVA with a blending ratio of 10:90 were selected for studying the possibility of nanofibers as pramipexole carriers. The optimum concentration of Kf, PVA, and CS solutions were 8%, 10%, and 3% W/V, respectively. After optimizing the electrospinning of Kf/CS/PVA nanofibers, pramipexole was chosen as a drug to study the drug delivery ability of kefiran composite nanofibers. To this end, 240 mg of drug was blended with Kf/CS/PVA solution due to the percentage of pramipexole in commercial non-nano patches [50]. The blended pramipexole/Kf/CS/PVA solution was electrospun at the condition the same as the Kf/CS/PVA electrospinning process. The electrospun pramipexole-loaded Kf/CS/PVA nanofibers were prepared and cross-linked with glutaraldehyde vapors (GTA) at room temperature. Figures 4.a and 4.b show the SEM image of pramipexole-loaded Kf/CS/PVA nanofibers and cross-linked pramipexole-loaded Kf/CS/PVA nanofibers, respectively. As can be seen in Fig. 4a, beadless and consistent nanofibrous morphology exists for the drug-loaded fibers with a mean diameter of 90 nm. A decrease was observed in the fiber diameter of the drug-loaded nanofibers compared to the Kf/CS/PVA nanofibers (125 nm).

The SEM images of cross-linked electrospun pramipexole-loaded Kf/CS/PVA nanofibers (Figure 4. b) with glutaraldehyde show the maintenance of nanofibrous structures while adhesion between nanofibers is observed, approving the cross-linking process. The increased diameter of the nanofibers (94 nm) is attributed to the adsorption of glutaraldehyde vapors into the nanofibrous structure. Furthermore, we investigated the potential of Kf/PVA composite nanofibers as a pramipexole carrier to compare them with Kf/CS/PVA composite nanofibers. In our previous work, modified Kf/PVA composite nanofibers containing [39] 8% PVA and 6% Kf polymer blend with the mixing ratio of Kf:PVA 40:60 was prepared and loaded with 240 mg pramipexole dihydrochloride; the nanofibers were then fabricated via the electrospinning process (electrospinning parameters were set as an applied voltage of 18 kV, 1 mL/h flow rate, and 200 mm tip-to-collector distance).

SEM micrographs, pramipexole-loaded Kf/PVA composite nanofibers, and GTA cross-linked pramipexole-loaded Kf/PVA composite nanofibers (Fig. 5) showed the successful fabrication of beadless, uniform fiber structures. The mean diameter of the fibers reduced from 90 nm in pramipexole-loaded Kf/CS/PVA nanofibers (Fig. 4a) to 58 nm in chitosan-free composite fibers (Fig. 5a). Adhesion was observed between nanofibers after crosslinking (Fig. 5b) while the nanofibrous morphology of the fibers stayed the same. The increased size of the fibers due to glutaraldehyde crosslinking was also evidenced (113 nm). Cross-linked pramipexole-loaded Kf/PVA composite nanofibers as larger in diameter (113 nm) than cross-linked pramipexole-loaded Kf/CS/PVA nanofibers (94 nm), proving that chitosan addition can decrease the ability to crosslink due to losing the brig structure of PVA crosslinking.

The AFM topographic images of pramipexole-

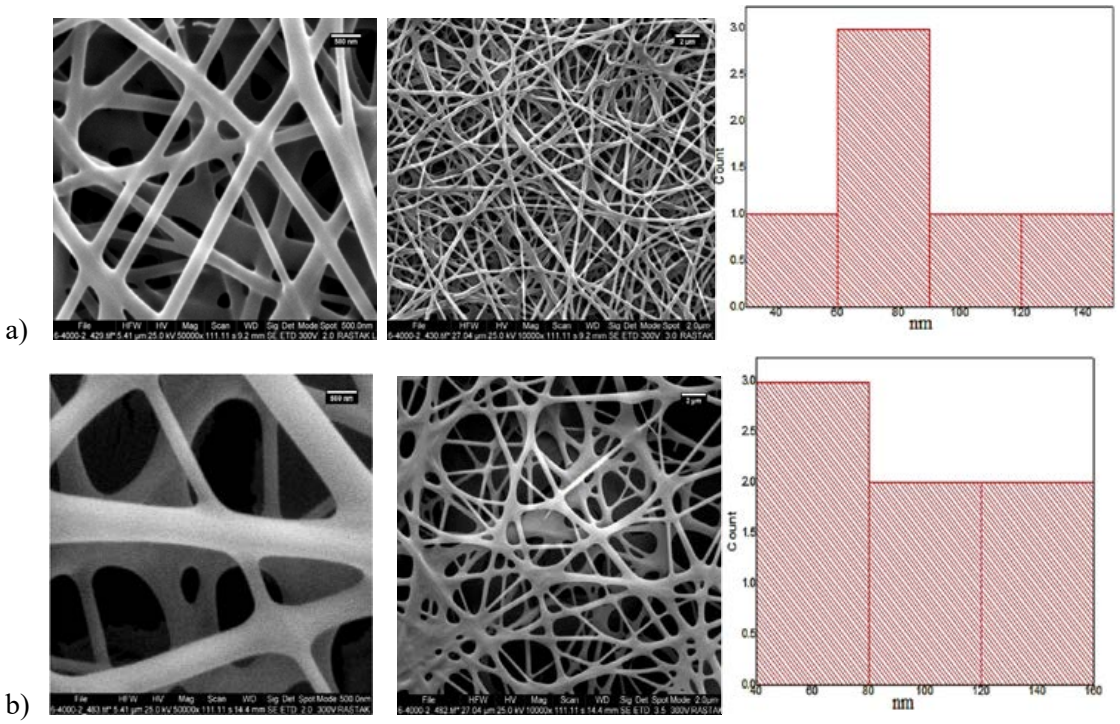

Fig. 4. SEM image (with different magnification, scale bar corresponds to 2 μm and 500 nm) and fiber diameter distribution of electrospun (a) pramipexole-loaded Kf/Cs/PVA nanofibers and (b) cross-linked pramipexole-loaded Kf/Cs/PVA nanofibers.

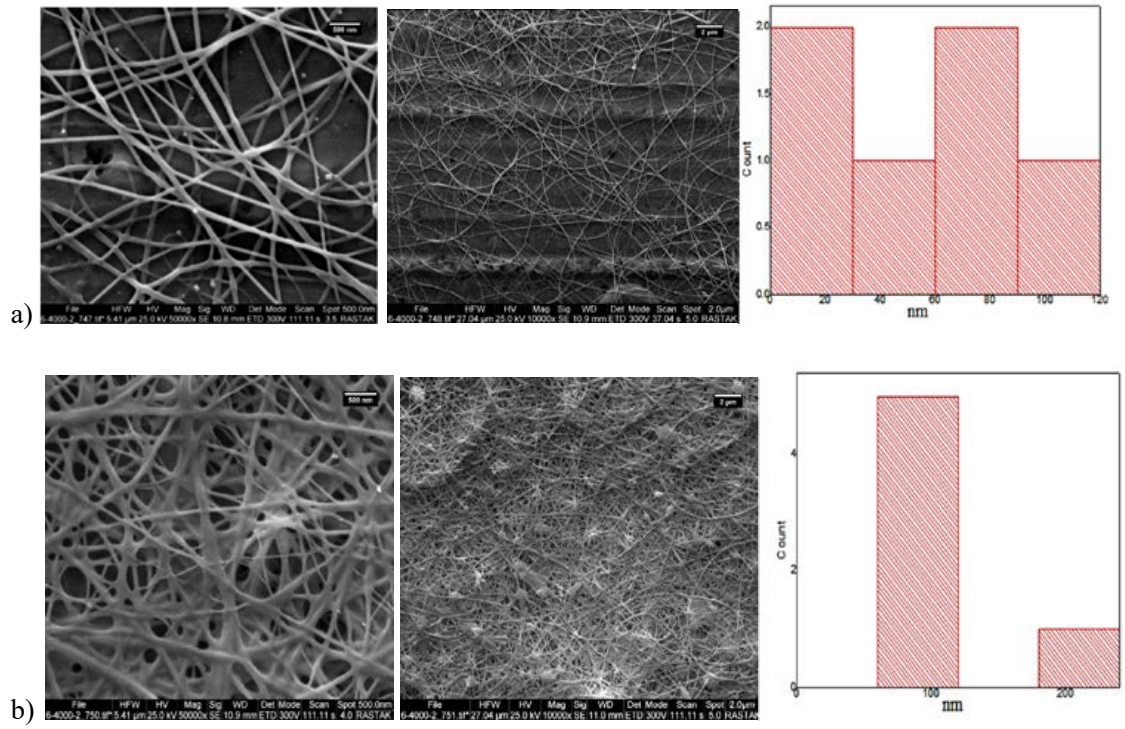

Fig. 5. SEM image (with different magnification, scale bar corresponds to 2 μm and 500 nm) and fiber diameter distribution of electrospun (a) pramipexole-loaded Kf/ /PVA nanofibers and (b) cross-linked pramipexole-loaded Kf/ PVA nanofibers.

loaded Kf/PVA, cross-linked pramipexole-loaded Kf/PVA, pramipexole-loaded Kf/CS/PVA, and cross-linked pramipexole-loaded Kf/PVA composite nanofibers are depicted in Fig. 6. Yet, due to the crosslinking adhesion, the 3D structure and nanofibrous morphology of the fibers were well-maintained after GTA crosslinking (Fig. 7.a and 7.b). AFM analyses revealed the nanofibrous morphology of the materials either in cross-linked or non-cross-linked frameworks (two nano-sized coordinates and a non-nano dimension along the xy-coordinates), though the adhesion between

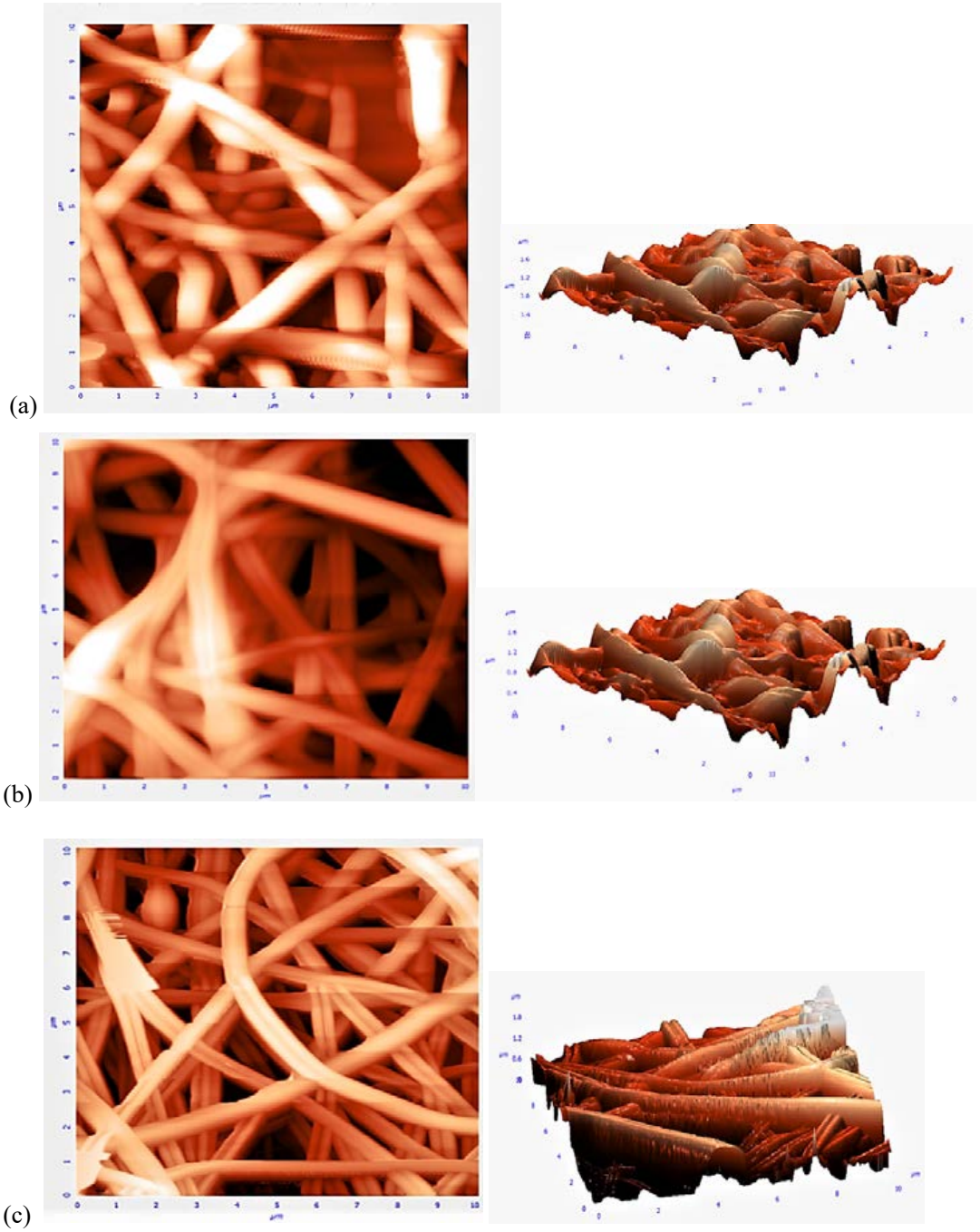

Fig. 6. AFM topographical images of pramipexole-loaded (a) Kf/PVA (b) cross-linked Kf/PVA (c) Kf/Cs/PVA and (d) crosslinked Kf/Cs/PVA nanofibers.

(d)

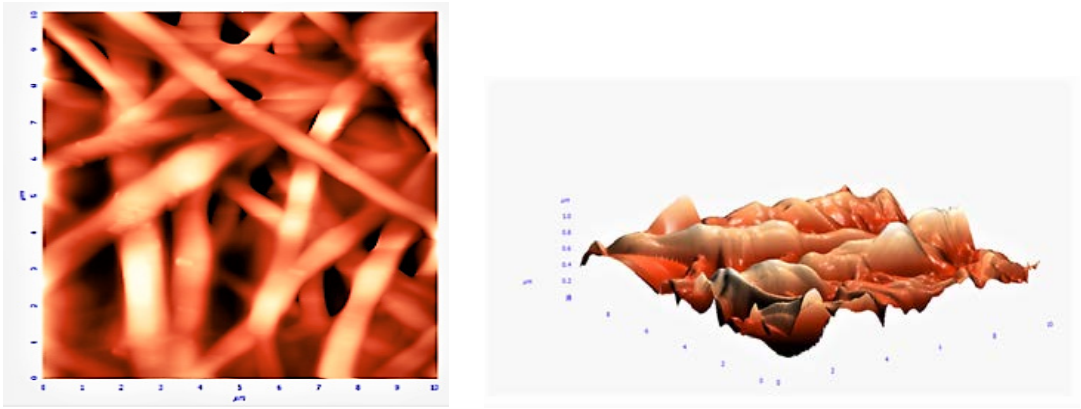

Continued Fig. 6. AFM topographical images of pramipexole-loaded (a) Kf/PVA (b) cross-linked Kf/PVA (c) Kf/Cs/PVA and (d) crosslinked Kf/Cs/PVA nanofibers.

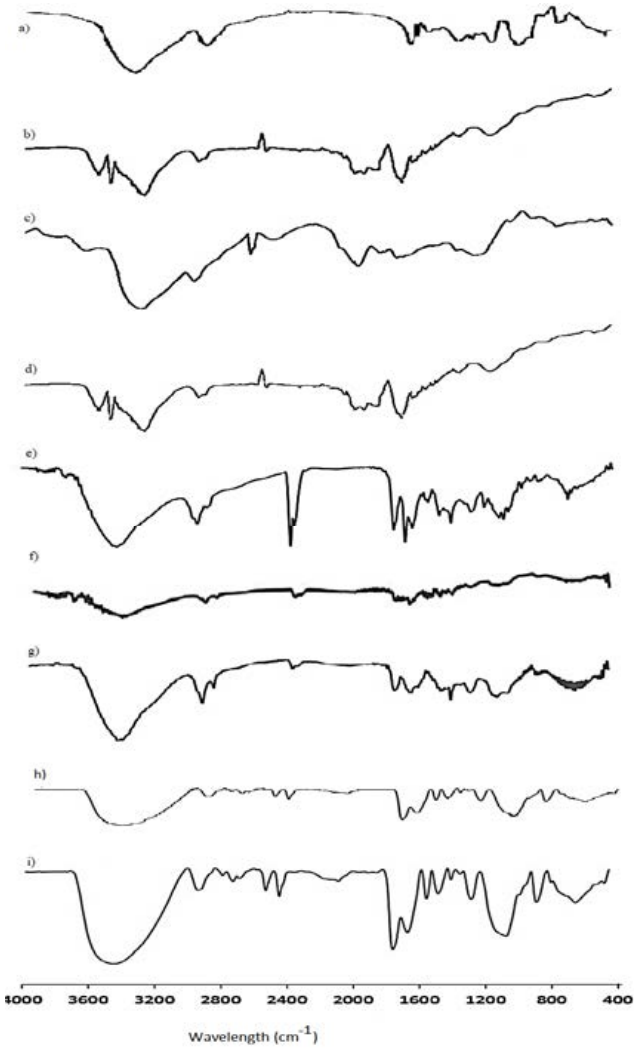

Fig. 7. FT-IR spectra of (a) pure PVA (b) pure Cs (c) purified kefiran biopolymer (d) Kf/PVA nanofibers (e) Kf/Cs/PVA nanofibers (f) pramipexole-loaded Kf/PVA nanofibers (g) cross-linked pramipexole-loaded Kf/PVA (h) pramipexole-loaded Kf/Cs/PVA and (i) cross-linked pramipexole-loaded Kf/Cs/PVA nanofibers.

nanofibers in cross-linked structure was observed as well (Fig. 4).

Fig. 7 shows the FT-IR spectra of pristine polymers, electrospun nanofibers of Kf/PVA and Kf/CS/PVA, pramipexole-loaded Kf/PVA, cross-linked pramipexole-loaded Kf/PVA, pramipexole-loaded Kf/CS/ PVA, and cross-linked pramipexole-loaded Kf/CS/PVA nanofibers, respectively. The pure PVA (Fig. 7a) showed different transmittance peaks at 813, 1226, 1353, 1535, 1724, 2875, and 3614 cm^{-1}, corresponding to the (C–C), (C–O), (CH), (CH–OAC), and (C=O) residual from primary vinyl acetate, (CH2), and free (OH) resonance, respectively, which is in agreement with the findings of previous research [50-51]. As indicated in the FT-IR spectrum of kefiran (Fig. 7.c), at the fingerprint region of 900-1200 cm^{-1}, characteristic absorption bands of kefiran polysaccharide including stretching modes of ring bonds and side groups (C-O-C, C-OH and C-H) and the vibration modes of glucose, galactose, and β-linkage were observed in the structure of pure kefiran [52]. Also, the peak at 1645 cm^{-1} is related to the bond of water [53]. Fig. 7b shows characteristic peaks of CS. The absorption peak at 1080 cm^{-1} was related to the C-O-C of the cyclic ether stretching of CS The amide-type II of CS appeared at 1558 cm^{-1}[54]. In addition, the absorption peaks around 1643 and 1687 cm^{-1} were attributed to C=O amid type I, the esteric group of CS [55]. The characteristic peaks at 2928 and 2956 cm^{-1} were related to CH_2 symmetric and asymmetric starching vibration. The presence of broad peaks at 3261, 3421, and 3443 cm^{-1} is a result of the stretching vibration of –OH and $–NH_2$ involving in the inter and intramolecular hydrogen bonding in CS [56]. The FT-IR spectrum of electrospun Kf/CS/ PVA nanofibers (Fig 7e) revealed the characteristic peaks of all the components as well as overtones of C=O stretching at 2360 cm^{-1}, around 2924 cm^{-1} for aliphatic C-H, and overtones of O-H stretching at 3440 cm^{-1}. The ATR-FTIR spectra of the cross-linked and non-cross-linked pramipexole-loaded Kf-PVA nanofibers demonstrated the successful incorporation of pramipexole into the fibers (Fig. 7.f, g). Absorption bands at 2921, 2850, 1440, 1320, 1242, 1095, and 850 cm^{-1} were attributed to CH, CH_2, C-C, C-O, CH, CHOH, and CH-OH, respectively. Broad bands above 3000 cm^{-1} are indicative of hydroxylic groups of polysaccharides and PVA polymer. The absorption bands at 1300-1800 cm^{-1} were ascribed to the stretching and bending vibrations of PVA polymer, and the bands at the fingerprint region complied with stretching modes of carbohydrates rings and their side chains. The characteristic peaks of PVA and kefiran were observed along with the overtone peaks of C=O stretching at 2360 cm^{-1}, aliphatic C-H around 2920 cm^{-1}, and the O-H stretching of both PVA and kefiran at 3440 cm^{-1}. The absorption bands at 3137, 3163, 3635, and 3751 cm^{-1} related to NH and NH_2 groups (1575cm^{-1} and 1238-1253 cm^{-1}assigned to N-H bending and C-N stretching of pramipexole) evidently demonstrated loading of the drug into the electrospun nanofibers. From the comparison of spectra of Kf/PVA (Fig. 7d) and Kf/Cs/PVA (Fig. 7e) with drug loaded composite nanofibers (Fig. 7f-7i), it can be concluded that the characteristic peaks of pramipexole, including 756, 839-945, 1133-1135, 1238-1253, 1533, 1575, 1714, 2324, 3163-3751 cm^{-1} that correspond to C-H bending, C-N bending, C=C bending, C-N stretching, ring C=N, N-H bending, phenyl nitro thiazole ring, aliphatic C-H stretching, NH and NH_2 stretching respectively, are evident in all spectra. Appearance of specified peaks related to pramipexol suggests the successful loading of drug and indicates that the integration of the drug with polymers followed by electrospinning did not change the structure of the drug or polymers.

The water contact angle of the cross-linked and non-cross-linked pramipexole-loaded Kf/PVA and Kf/CS/PVA nanofibers were measured (Fig. 8). As can be seen in Fig.s 8.a and 8.b, the water contact angle of pramipexole-loaded Kf/PVA and cross-linked pramipexole-loaded Kf/PVA were 43° and 65°, respectively. The higher contact angle of cross-linked nanofibers revealed the increased hydrophobicity of the material after being cross-linked owing to the entanglement of hydroxyl groups in the acetal bonds of PVA. This medium wettability is considered to have a great potential for using the drug on the skin due to the extended release of the drug on the amphiphilic structure of skin. Wettability also decreased by the GTA cross-linking of the Kf/CS/PVA nanofibers (Fig. 8.c and 8.d) leading to an increased contact angle (water contact angle of 55° for cross-linked pramipexole-loaded Kf/CS/PVA nanofibers compared to the contact angle of 33°). The water contact angle of cross-linked pramipexole-loaded Kf/CS/PVA nanofibrous mats was indicative of the typical hydrophilic nature of the fibers (Fig. 8). The contact angle of drug-loaded Kf/CS/PVA

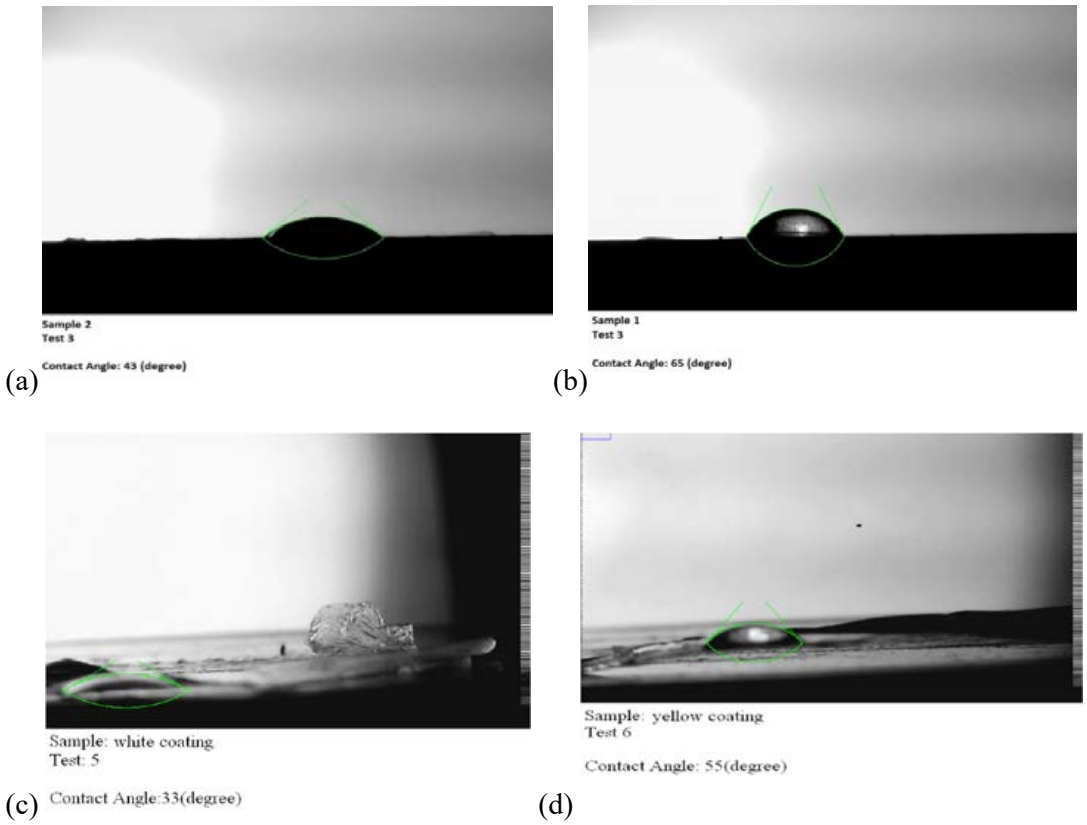

Fig. 8. Water contact angle of electrospun nanofibers of pramipexole-loaded (a) Kf/PVA (b) cross-linked Kf/PVA (c) PVA/Cs/Kf nanofibers d) cross-linked PVA-Cs-Kf nanofibers

nanofibers was lower than corresponding Kf/PVA nanofibers because of the presence of chitosan as a hydrophobic polymer.

In vitro dissolution measurements were employed to determine the drug release features of cross-linked and non-cross-linked pramipexole-loaded nanofibers using a dissolution apparatus (phosphate buffered saline pH 7.4 as a solvent, 37 °C). Pramipexole concentration in the samples was measured at specific intervals via UV-Visible spectroscopy. Standard solutions of 1, 2, 5, 10, 15, 20, and 25 ppm were prepared, and absorbencies were recorded at the maximum wavelength of 263 nm at 25° C to draw and calibration curve of standard solutions (Fig. 9). The amount of pramipexole in nanofibril samples was calculated using the calibration curve of standard solutions.

Fig. 10 depicts the drug-loaded, electrospun nanofibers' release profile. The drug release percentage was calculated given the maximum drug release of 40 mg in 13×5 cm pieces of nanofibrous mats.

Fig. 10.a shows the release behavior of pramipexole-loaded Kf/PVA nanofibers. As can be seen, during the first five minutes of immersion, 18% of the drug was released and reached 24% after 48 hours. The maximum amount of drug release and reaching a steady state occurred after 56 hours. Dadashi et al [45] loaded doxycycline in kefiran nanofibers and study release behavior and antibacterial effect of doxycycline/Kef nanofibers. The maximum amount of drug released from doxycycline/Kef nanofibers was about 45% of the loaded drug over 96 h with 30% burst release in 5 h. Strong hydrogen bonding between drug, PVA, and kefiran is supposed to resist the solvation of the drug in water led to very slower and lower release behavior of Kf/PVA nanofibers than Kf nanofibers.

Compared to non-cross-linked pramipexole-loaded Kf/PVA nanofibers, cross-linked drug-loaded Kf/PVA nanofibers had a slower initial release, but the percentage of the release was closed and followed the same behavior with a 3-5% decrease in the total release of the drug. As

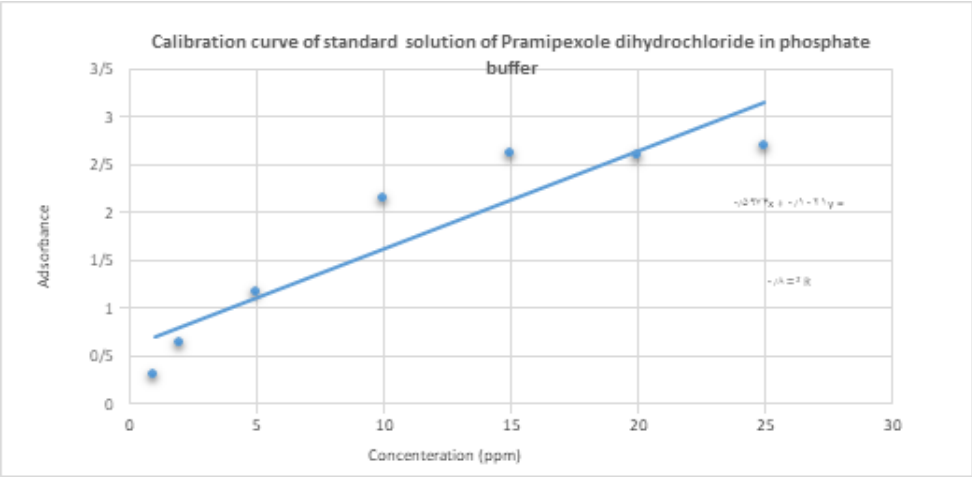

Fig. 9. Calibration curve of pramipexole standard solutions in phosphate buffer pH 7.4.

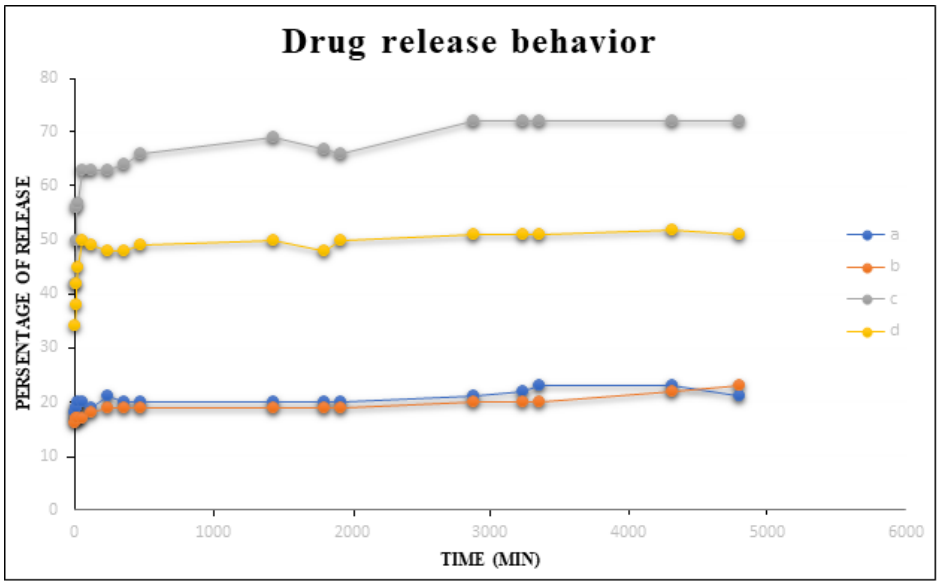

Fig. 10. Drug release behavior of pramipexole-loaded (a) Kf/PVA nanofibers (b) cross-linked Kf/PVA nanofibers (c) Kf/Cs/PVA nanofibers (d) cross-linked Kf/Cs/PVA nanofibers.

indicated in Fig. 10.c, about 40% of pramipexole was released in five minutes after the immersion of electrospun pramipexole-loaded Kf/CS/PVA nanofibers. The release of the drug kept increasing at a slow rate and reached the maximum amount of 75% of loaded drug after 72 hours that is higher than Kf/PVA nanfibers with 21% release after 72 h. It may be due to the high level of hydrogen bonding between PVA and drug which limits the release of drug in Kf/PVA nanofibers. While in the presence of chitosan, these bonds are more between polymers and the hydrophobic properties of chitosan lead to more drug release in Kf/CS/PVA nanofibers.

The *in-vitro* pramipexole release in crosslinked electrospun pramipexole-loaded Kf/CS/PVA nanofibers started five minutes after immersion with a 34% release and reached 53% in 72 hours. The maximum release and reaching a steady state took four days in total which can be attributed to the protection of the drug in the cross-linked

structure, causing a sustained release of the drug over time. The formation of acetal bonds between the hydroxyl groups of polymers and the carbonyl groups of glutaraldehyde blocked the hydroxyl groups. Consequently, this reduced the wettability, permeability, and solubility of the PVA substrate, resulting in a sustained drug release in drug-loaded nanofibers. Therefore, as opposed to the positive influence of crosslinking on the release behavior of pramipexole-loaded nanofibers, nanofibers' crosslinking led to a decrease in the drug release percentage and the initial release, hence a better choice for sustained-release drug delivery systems than non-cross-linked nanofibers. Thus, the reported experimental data in this study suggest that Kf/CS/PVA is a better drug carrier than Kf/PVA nanofibers because of its more sufficient, sustained, and controlled drug release power due to more controlled polarity properties of polymers with the addition of chitosan which can control diffusion, solubility, and release of nanofibers mat as a drug carrier.

CONCLUSION

Kf/CS/PVA composite nanofibers and kefiran/PVA composite nanofibers were synthesized by electrospinning method. The concentration of Kf, mixing ratio of Kf with CS/PVA and electrospinning condition were optimized by analyzing the SEM image of nanofibers. SEM images approved that 10% PVA, 3% CS, and 8% kefiran with 10:90 mixing ratio of Kf:CS/PVA, the electrospinning voltage of 15 kV, 0.5 mL/h flow rate, and a 100 mm tip-to-collector distance were the optimum condition for fabrication of Kf/CS/PVA composite nanofibers.

The nanofibers of pramipexole-loaded Kf/PVA and promipexole-loaded Kf/CS/PVA were fabricated in the optimum condition led to smooth and fine nanofibers with the average diameter of 58 nm and 90 nm respectively. Drug-loaded nanofibers were cross-linked using glutaraldehyde vapors. The SEM images showed an average diameter of 113 nm and 94 nm for GTA cross-linked pramipexole-loaded Kf/PVA and Kf/CS/PVA nanofibers respectively. Water contacts angle analysis demonstrated the increased hydrophobicity of the fibers by cross-linking. The release behavior of all drug-loaded nanofibers were studying using *in vitro* dissolution procedure and UV-Visible spectroscopy. Kf/PVA nanofibers showed slow and low drug release properties in contrast to Kf/CS/PVA nanofibers. Although crosslinked composite nanofibers had slower release behavior than their non-cross-linked counterparts which can be ascribed to the formation of acetal bonds and a decrease in the content of free hydroxylic groups of the composite nanofibers.

ACKNOWLEDGMENT

The authors are grateful to the Active Pharmaceutical Ingredients Research Center (APIRC) and the Pharmaceutical Sciences Research Center, Tehran Medical Sciences, Islamic Azad University for providing laboratory equipment and services.

FUNDING

This research received no grant from any funding organizations.

CONFLICT OF INTEREST

The corresponding authors had no conflict of interest.

REFERENCES

1. Bhargava Reddy MS, Ponnamma D, Choudhary R, Sadasivuni KK .A Comparative Review of Natural and Synthetic Biopolymer Composite Scaffolds. Polymers, 2021;13:1105. https://doi.org/10.3390/polym13071105
2. Ziting B, Caihong X, Qijuan Y, Guiting L, Jun W. Natural Polymer-Based Hydrogels with Enhanced Mechanical Performances: Preparation, Structure, and Property. Adv. Healthcare Mater. 2019;8:e1900670. https://doi.org/10.1002/adhm.201900670
3. Nangai EK, Saravanan S. Synthesis, fabrication and testing of polymer nanocomposites: A review. Materials today, proceedings, 2021. https://doi.org/10.1016/j.matpr.2021.02.261 https://doi.org/10.1016/j.matpr.2021.02.261
4. Boreddy SR Reddy (eds) Advances in diverse industrial applications of nanocomposites (India: Intech) 2011. https://doi.org/10.5772/1931
5. Sharma S, Malik A and Gupta P in S Ahmed and Annu (eds) Bionanocomposites in tissue engineering and regenerative medicine (Woodhead Publishing) 2021;P 507. https://doi.org/10.1016/C2019-0-03520-0
6. Akbar MU, Athar MM, Bhatti IA, Bhatti HN, Khosa MK, Zia KM and et al Chapter 17 - Biomedical applications of bionanocomposites, KM Zia et al (eds) In Micro and Nano Technologies, Bionanocomposites (Elsevier) 2020;457-483. https://doi.org/10.1016/B978-0-12-816751-9.00017-9
7. Arora B, Bhatia R and Attri P 28 - Bionanocomposites: Green materials for a sustainable future,
in CM Hussain and AK Mishra (eds) New Polymer Nanocomposites for Environmental Remediation (Elsevier) 2018;699-712. https://doi.org/10.1016/B978-0-12-811033-1.00027-5
8. Zafar R, Zia KM, Tabasum S, Jabeen F, Noreen A, Zuber M. Polysaccharide based bionanocomposites, properties and applications: A review. Int. J. Biol. Macromol. 2016;92:1012-1024. https://doi.org/10.1016/j.ijbiomac.2016.07.102
9. Radhouani H, Bicho D, Gonçalves C, Maia FR, Reis RL,

Oliveira JM. Kefiran cryogels as potential scaffolds for drug delivery and tissue engineering applications. Materials Today Communications, 2019;20:100554. https://doi.org/10.1016/j.mtcomm.2019.100554
10. Ghasemlou M, Khodaiyan F, Oromiehie A, Yarmand MS. Development and characterisation of a new biodegradable edible film made from kefiran, an exopolysaccharide obtained from kefir grains. Food Chemistry, 2011;127:1496-1502. https://doi.org/10.1016/j.foodchem.2011.02.003
11. Piermaria J, Diosma G, Aquino C, Garrote G, Abraham A. Edible kefiran films as vehicle for probiotic microorganisms. Innovative Food Science & Emerging Technologies, 2015;32:193-199. https://doi.org/10.1016/j.ifset.2015.09.009
12. Moradi Z, Kalanpour N, Kefiran, a branched polysaccharide: Preparation, properties and applications: A review. Carbohydrate Polymers, 2019;223:115100. https://doi.org/10.1016/j.carbpol.2019.115100
13. Bengoa AA, Dardis C, Gagliarini N, Garrote GL, Abraham AG. Exopolysaccharides from Lactobacillus paracasei isolated From Kefir as Potential Bioactive Compounds for Microbiota Modulation. Frontiers in Microbiology, 2020;11:583254. https://doi.org/10.3389/fmicb.2020.583254
14. Blandón LM, Noseda MD, Islan GA, Castro GR, de Melo Pereira GV, Thomaz-Soccol V, Soccol CR. Optimization of culture conditions for kefiran production in whey: The structural and biocidal properties of the resulting polysaccharide. Bioactive Carbohydrates and Dietary Fibre, 2018;16:14-21. https://doi.org/10.1016/j.bcdf.2018.02.001
15. Riaz Rajoka MS, Mehwish HM, Fang H, Padhiar AA, Zeng X, Khurshid M, He Z, Zhao L. Characterization and anti-tumor activity of exopolysaccharide produced by Lactobacillus kefiri isolated from Chinese kefir grains. Journal of Functional Foods, 2019;63:103588. https://doi.org/10.1016/j.jff.2019.103588
16. Jeong D, Kim DH, Kang IB, Kim H, Song KY, Kim HS, Seo KH. Characterization and antibacterial activity of a novel exopolysaccharide produced by Lactobacillus kefiranofaciens DN1 isolated from kefir. Food Control, 2017;78:436-442. https://doi.org/10.1016/j.foodcont.2017.02.033
17. Luang-In V, Deeseenthum S. Exopolysaccharide-producing isolates from Thai milk kefir and their antioxidant activities. LWT. 2016;73:592-601. https://doi.org/10.1016/j.lwt.2016.06.068
18. Prado MRM, Boller C, Zibetti RGM, de Souza D, Pedroso LL, Soccol CR. Anti- inflammatory and angiogenic activity of polysaccharide extract obtained from Tibetan kefir. Microvascular Research, 2016;108:29-33. https://doi.org/10.1016/j.mvr.2016.07.004
19. Cevikbas A, Yemni E, Ezzedenn FW, Yardimici T, Cevikbas U, Stohs S. Antitumoural antibacterial and antifungal activities of kefir and kefir grain. Phytotherapy Research, 1994;8:78-82. https://doi.org/10.1002/ptr.2650080205
20. Rodrigues KL, Caputo LRG, Carvalho JCT, Evangelista J, Schneedorf JM. Antimicrobial and healing activity of kefir and kefiran extract. International journal of antimicrobial agents, 2005;25:404-408. https://doi.org/10.1016/j.ijantimicag.2004.09.020
21. Hamida RS, Shami A, Ali MA, Almohawes ZN, Mohammed AE, Bin-Meferij MM. Kefir: A protective dietary supplementation against viral infection. Biomedicine & Pharmacotherapy, 2021;133:110974-110985. https://doi.org/10.1016/j.biopha.2020.110974
22. Piermaría J, Bengoechea C, Abraham AG, Guerrero A. Shear and extensional properties of kefiran. Carbohydrate Polymers, 2016;152:97-104. https://doi.org/10.1016/j.carbpol.2016.06.067
23. Exarhopoulos S, N. Raphaelides S, G. Kontominas M. Conformational studies and molecular characterization of the polysaccharide kefiran. Food Hydrocolloids, 2018;77:347-356. https://doi.org/10.1016/j.foodhyd.2017.10.011
24. Piermaria JA, de la Canal ML, Abraham AG. Gelling properties of kefiran, a food-grade polysaccharide obtained from kefir grain. Food Hydrocolloids, 2008;22:1520-1527. https://doi.org/10.1016/j.foodhyd.2007.10.005
25. Piermaria J, Bosch A, Pinotti A, Yantorno O, Garcia MA, Abraham AG. Kefiran films plasticized with sugars and polyols: water vapor barrier and mechanical properties in relation to their microstructure analyzed by ATR/FT-IR spectroscopy. Food Hydrocolloids, 2011;25:1261-1269. https://doi.org/10.1016/j.foodhyd.2010.11.024
26. Motedayen AA, Khodaiyan F, Salehi EA. Development and characterisation of composite films made of kefiran and starch. Food Chemistry, 2013;136:1231-1238. https://doi.org/10.1016/j.foodchem.2012.08.073
27. Zolfi M, Khodaiyan F, Mousavi M, Hashemi M. Development and characterization of the kefiran-whey protein isolate-TiO2 nanocomposite films. International Journal of Biological Macromolecules, 2014;65:340-345. https://doi.org/10.1016/j.ijbiomac.2014.01.010
28. Piermaria JA, Pinotti A, Garcia MA, Abraham AG. Films based on kefiran, an exopolysaccharide obtained from kefir grain: Development and characterization. Food Hydrocolloids, 2009;23:684-690. https://doi.org/10.1016/j.foodhyd.2008.05.003
29. Rad FH, Sharifan A, Asadi G. Miscibility and morphology of kefiran/waterborne polyurethane blend films. International Journal of Food Properties, 2017;20:S2764-S2775. https://doi.org/10.1080/10942912.2017.1373664
30. Esnaashari SS, Rezaei S, Mirzaei E, Afshari H, Rezayat SM, Faridi-Majidi R. Preparation and characterization of kefiran electrospun nanofibers. International Journal of Biological Macromolecules, 2014;70:50-56. https://doi.org/10.1016/j.ijbiomac.2014.06.014
31. Jenab A, Roghanian R, Ghorbani N, Ghaedi K, & Emtiazi G. The Efficacy of Electrospun PAN/Kefiran Nanofiber and Kefir in Mammalian Cell Culture: Promotion of PC12 Cell Growth, Anti- MCF7 Breast Cancer Cells Activities, and Cytokine Production of PBMC. International Journal of Nanomedicine, 2020;15:717-728. https://doi.org/10.2147/IJN.S232264
32. Jenab A, Roghanian R, Emtiazi G, Ghaedi K. Manufacturing and structural analysis of antimicrobial kefiran/polyethylene oxide nanofibers for food packaging. Iranian Polymer Journal, 2017;26:31-39. https://doi.org/10.1007/s13726-016-0496-7
33. Aslam M, Kalyar MA, Raza ZA. Polyvinyl Alcohol: A Review of Research Status and Use of Polyvinyl Alcohol Based Nanocomposites. Polymer Engeeneering and Science. 2018;58:2119-2132. https://doi.org/10.1002/pen.24855
34. Ben Halima N. Poly (vinyl alcohol): review of its promising applications and insights into biodegradation. RSC Advances. 2016;6:39823-39832. https://doi.org/10.1039/C6RA05742J
35. Marin Cardona Es, Rojas Camargo J, Ciro Monsalve YA. A review of polyvinyl alcohol derivatives: Promising materials for pharmaceutical and biomedical applications. African Journal of Pharmacy and Pharmacology, 2013;8:674-684.

https://doi.org/10.5897/AJPP2013.3906
36. Gaaz TS, Sulong AB, Akhtar MN, Kadhum AAH, Mohamad AB, Al-Amiery AA. Properties and applications of polyvinyl alcohol, halloysite nanotubes and their nanocomposites. Molecules, 2015;20:2833-22847. https://doi.org/10.3390/molecules201219884
37. Saini I, Sharma A, Dhiman R, Aggarwal S, Ram S, Sharma PK. Grafted SiC nanocrystals: For enhanced optical, electrical and mechanical properties of polyvinyl alcohol. Journal of Alloys Compounds, 2017;714:172-180. https://doi.org/10.1016/j.jallcom.2017.04.183
38. Lu W, Yao J, Zhu X, Qi Y. Nanomedicines: Redefining traditional medicine. Biomedicine & Pharmacotherapy, 2021;134:111103. https://doi.org/10.1016/j.biopha.2020.111103
39. Mina bagherian far, Hakimeh Ziyadi. Fabrication of Polyvinyl Alcohol/Kefiran Nanofibers Membrane Using Electrospinning. Journal of Pharmaceutical and Health Sciences, 2016;4(3):211-218.
40. Mehrali F, Ziyadi H, Hekmati M, Faridi-Majidi R, Qomi M. Kefiran/poly(vinyl alcohol)/poly(vinyl pyrrolidone) composite nanofibers: fabrication, characterization and consideration of effective parameters in electrospinning. SN Applied Sciences, 2020;2:895. https://doi.org/10.1007/s42452-020-2714-3
41. Shokraei S, Mirzaei E, Shokraei N, Derakhshan MA, Ghanbari H, Faridi-Majidi R. Fabrication and characterization of chitosan/kefiran electrospun nanofibers for tissue engineering applications. applied polymer science. 2021; 138:50547. https://doi.org/10.1002/app.50547
42. Azmana M, Mahmood S, Hilles AR, Rahman A, Arifin MAB, Ahmed S. A review on chitosan and chitosan-based bionanocomposites: Promising material for combatting global issues and its applications. International Journal of Biological Macromolecules, 2021;185:832-848. https://doi.org/10.1016/j.ijbiomac.2021.07.023
43. Khan A, Alamry KA . Recent advances of emerging green chitosan-based biomaterials with potential biomedical applications: A review. Carbohydrate Research, 2021;506:108368. https://doi.org/10.1016/j.carres.2021.108368
44. Liang H, Mirinejad MS, Asefnejad A, Baharifar H, Li X, Saber-Samandari S, ... & Khandan A. Fabrication of tragacanthin gum-carboxymethyl chitosan bio-nanocomposite wound dressing with silver-titanium nanoparticles using freeze-drying method. Materials Chemistry and Physics, 2022;279:125770. https://doi.org/10.1016/j.matchemphys.2022.125770
45. Raisi A, Asefnejad A, Shahali M, Doozandeh Z, Kamyab Moghadas B, Saber-Samandari S, & Khandan A. A soft tissue fabricated using a freeze-drying technique with carboxymethyl chitosan and nanoparticles for promoting effects on wound healing. Journal of Nanoanalysis, 2020;7(4):262-274. https://doi.org/10.22034/JNA.2022.680836
46. Jamnezhad S, Asefnejad A, Motififard M, Yazdekhasti H, Kolooshani A, Saber-Samandari S, & Khandan A. Development and investigation of novel alginate-hyaluronic acid bone fillers using freeze drying technique for orthopedic field. Nanomedicine Research Journal, 2020;5(4):306-315. https://doi.org/10.22034/nmrj.2020.04.00
47. Sabaghi M, Maghsoudlou Y, Habibi P. Enhancing structural properties and antioxidant activity of kefiran films by chitosan addition. Food Structure, 2015;5:66-71. https://doi.org/10.1016/j.foostr.2015.06.003
48. Dadashi S, Boddohi S, Soleimani N. Preparation, characterization, and antibacterial effect of doxycycline loaded kefiran nanofibers. Journal of Drug Delivery Science and Technology, 2019;52:979-985. https://doi.org/10.1016/j.jddst.2019.06.012
49. M. Blandón L, A. Islan G, R. Castro G, D. Noseda M, Thomaz-Soccol V, R. Soccol C. Kefiran-alginate gel microspheres for oral delivery of ciprofloxacin, Colloids and Surfaces B: Biointerfaces, 2016;145:706-715. https://doi.org/10.1016/j.colsurfb.2016.05.078
50. Moreno-Cortez IE, Romero-García J, González-González V, García-Gutierrez DI, Garza-Navarro MA, Cruz-Silva R. Encapsulation and immobilization of papain in electrospun nanofibrous membranes of PVA cross-linked with glutaraldehyde vapor. Mater. Sci. Eng. C, 2015;52:306-314. https://doi.org/10.1016/j.msec.2015.03.049
51. Nadem S, Ziyadi H, Hekmati M, baghali M. Cross-linked poly (vinyl alcohol) nanofibers as drug carrier of clindamycin. Polymer Bulletin, 2020;77:5615-5629. https://doi.org/10.1007/s00289-019-03027-z
52. Piermaria J, Bosch A, Pinotti A, Yantorno O, Garcia MA, Abraham AG. Kefiran films plasticized with sugars and polyols: water vapor barrier and mechanical properties in relation to their microstructure analyzed by ATR/FT-IR spectroscopy. Food Hydrocolloid, 2011;25:1261-1269. https://doi.org/10.1016/j.foodhyd.2010.11.024
53. Ghasemlou M, Khodaiyan F, Jahanbin K, Garibzahedi SMT, Taheri S. Structural investigation and response surface optimisation for improvement of kefiran production yield from a low-cost culture medium. Food chem. 2012;133:383-389. https://doi.org/10.1016/j.foodchem.2012.01.046
54. Archana D, Dutta J, Dutta PK. Evaluation of chitosan nano dressing for wound healing: Characterization, in vitro and in vivo studies, International journal of biological macromolecules, 2013;57:193-203. https://doi.org/10.1016/j.ijbiomac.2013.03.002
55. Papich MG. Saunders handbook of veterinary drugs, (Elsevier) 2007:236-238.
56. Kacurakova M, Capek P, Sasinkova V, Wellner N, Ebringerova A. FT-IR study of plant cell wall model compounds: pectic polysaccharides and hemicelluloses. Carbohydrate polymers, 2000;43:195-203. https://doi.org/10.1016/S0144-8617(00)00151-X